Reducing B1 Inhomogeneity Using Optimized Parallel Transmit Pulses

D. Xu[1], K. F. King[2], G. McKinnon[2], and Z-P. Liang[1]

[1]Electrical and Computer Engineering, University of Illinois at Urbana-Champaign, Urbana, IL, United States, [2]General Electric Healthcare, Milwaukee, WI, United States

INTRODUCTION

Inhomogeneous B_1 field can cause serious image shading in high field imaging. Static RF shimming with a multi-port transmit coil array [1] has been proposed, which allows independent adjustment of the phase and amplitude of the otherwise identical pulse waveforms for the individual ports. More recently, parallel transmit [2-4] has been proposed to offer complete control over individual RF waveforms, and therefore is able to produce more homogeneous B_1 field [5]. However, the existing parallel-transmit pulse designs are based on small-tip-angle (STA) [2-4] or linear-class large-tip-angle (LCLTA) [6] approximations of the Bloch equation. When the assumptions associated with these methods are violated, the effectiveness to correct B_1 inhomogeneity can be significantly reduced. In [7], we propose to use a multidimensional, multi-controller, optimal control approach (OC) to optimize STA or LCLTA pulses. In this paper, we show various simulation results to demonstrate the effectiveness of this method to correct for B_1 inhomogeneity.

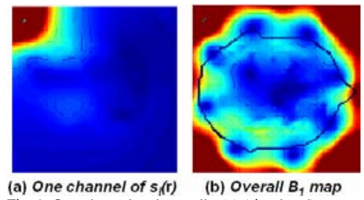

Fig. 1. One channel and overall $s_l(\mathbf{r})$ (simulated).

METHODS

We used FDTD software to simulate a transmit array of eight equidistant, radially oriented loops (1.5 × 16 cm^2) placed on a cylindrical coil former (diameter = 30 cm, length = 16 cm) with a 7 T main field strength. The numerical coil load was provided by segmented visible-man data [8], using appropriate electrical properties for various tissue types. The magnitude of one channel of the transmit sensitivities ($s_l(\mathbf{r})$, where l denotes the coil index and $\mathbf{r}$ denotes spatial location) is shown in Fig. 1a. The overall B_1 map (sum of $s_l(\mathbf{r})$ over all coils) is quite inhomogeneous (Fig 1b). Bloch simulations without relaxation were done to compare nonoptimized (LCLTA/STA) and optimized (OC) pulses. For simplicity, we normalized magnetizations by equilibrium magnetization M_0 so that a unity value corresponds to M_0.

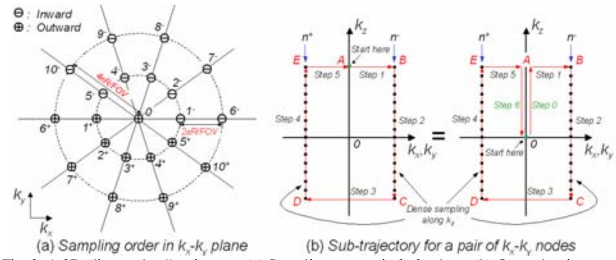

Fig. 2. A 3D "linear-class" trajectory. (a) Sampling pattern in k_x-k_y plane. (b) One subtrajectory.

2D 90° Excitation Pulses at Various Accelerations: This study was to compare the nonoptimized and optimized 2D parallel-transmit 90° excitation pulses for B_1 inhomogeneity correction at various acceleration factors (R = 1, 2, and 4). We first designed an STA pulse using the method in [4] to target for a homogeneous magnetization across a field-of-view (FOV) of 25 × 25 cm^2. Inward spiral excitation k-space trajectories with 20/R turns were used for the R-fold accelerated pulse (pulse duration T = 5/R msec). Initial magnetization vectors pointed to +z axis. Since there were large variations of $s_l(\mathbf{r})$ at the four corners of the FOV and these corners were outside of the object (e.g., a brain as depicted in Fig. 1b), we used spatial weights [7] that have unity value inside the circle $\Omega = \{x^2 + y^2 \le (12.5)^2\}$ and zero outside for the OC method. We measured inhomogeneity by mean value (μ) and standard deviation (σ) of M_y inside Ω.

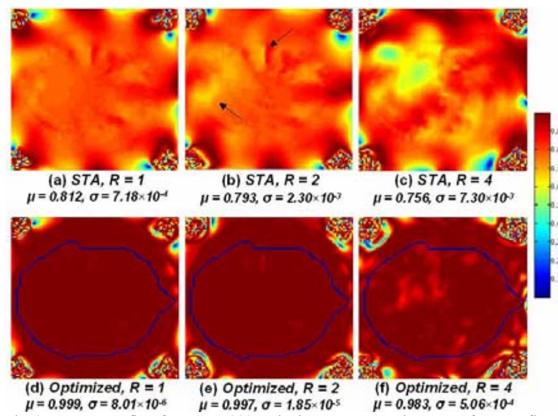

Fig. 3. (a-c) M_y profiles from STA 90° excitation pulses at various R. (d-f) M_y profiles from the corresponding optimized pulses.

3D 180° Slice-Selective Refocusing Pulse: In this study, we compared the results by a 3D parallel-transmit 180° refocusing pulse designed by the LCLTA method [6] and its optimized version. The initial magnetization vectors pointed to +y axis. The desired flip angle was 180° inside a 2 cm slice along the z axis and zero outside, and homogeneous in the x-y plane. Note that the k-space trajectory for the design of LCLTA pulses needs to satisfy the "linear class" condition, which means that the trajectory needs to be decomposable into inherently refocused sub-trajectories. We report one such 3D trajectory based on the fast-k_z trajectory [9]. Similarly to the original fast-k_z trajectory, the proposed trajectory covers k_z extensively to achieve slice selectivity and k_x-k_y plane sparsely to correct for the smooth nonuniformity of transmit sensitivity. As shown in Fig. 2a, samples in the k_x-k_y plane are concentrically distributed, where each ⊖ or ⊕ represents an inward or outward spoke of samples along k_z, and the circles are located at integer multiples of 2πR/FOV. The trajectory starts from the origin and sequentially visit the spokes in the order 0–1^-–1^+–2^-–2^+– ··· –N_s^-–N_s^+, where N_s is the number spokes. Visiting each (n^-,n^+)-pair constitutes a sub-trajectory, which follows an A-B-C-D-E-A order as shown in the left diagram of Fig. 2b. Each sub-trajectory is equivalent to an inherently refocused trajectory shown in the right diagram of Fig. 2b, which includes additional paths from origin to A and A back to origin (whose effects cancel each other). We used the unaccelerated trajectory with two circles, N_s = 10, and 24 samples along k_z for the simulation. FOV = 24 × 24 × 12 cm^3 and T = 5 msec. We measure the inhomogeneity inside the slice by mean value (μ), standard deviation (σ), and maximum difference of M_y.

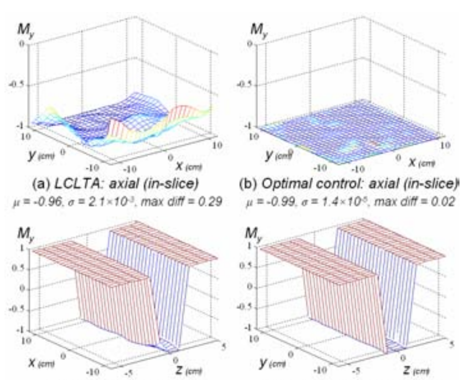

Fig. 4. (a-b) Axial views (in-slice) of M_y using LCLTA and optimized 3D refocusing pulses, and (c-d) the corresponding coronal views.

RESULTS

2D 90° Excitation Pulses at Various Accelerations: Figures 3a-c show the M_y profile after applying the STA pulses at various R. Although M_y from the unaccelerated pulse is quite uniform, some nonuniformity (marked by the arrows in Fig. 3b) starts to appear for the twofold acceleration case, and the nonuniformity becomes more severe for the fourfold accelerattion case. The mean values of M_y profiles for all STA pulses are significantly less than one (the target value), implying smaller flip angles actually achieved by these pulses. This is because the STA assumption does not quite hold for the 90° flip angle. The M_y profiles from the corresponding optimized pulses are shown in Figs. 3d-f. Much more uniform profiles are achieved for all acceleration factors (see caption for detailed comparison of σ). Notably, M_y profiles generated by the twofold and fourfold accelerated optimized pulses are even more uniform that that by the unaccelerated STA pulse. The mean signal values are close to one, indicating that 90° flip angles are achieved for most locations inside the FOV.

3D 180° Slice-Selective Refocusing Pulse: As shown in Fig. 4a, with the LCLTA pulse, magnetizations are flipped approximately 180° in the slice, but variations of M_y across the x-y plane are still noticeable. This was well corrected by the optimized pulse, as shown in Fig. 4b (detailed inhomogeneity parameters shown in the figure). The above observation was further confirmed by a coronal view of the resulting 3D M_y profiles (Figs. 4c-d).

CONCLUSION

Bloch simulation results on various parallel transmit pulses (excitation/refocusing, 2D/3D, various R) have shown that the optimal control method in [7] can be used to improve the performance of the linear methods (STA and LCLTA methods) in B_1 inhomogeneity correction applications at high field.

REFERENCES

[1] Ibrahim et al., *MRI*, vol. 18, pp. 733-742, 2000.
[2] Katscher et al., *MRM*, vol. 49, pp. 144-150, 2003.
[3] Y. Zhu, *MRM*, vol. 51, pp. 775-784, 2004.
[4] W. A. Grissom et al., *Proc. ISMRM*, pp. 19, 2005.
[5] Katscher et al., *Proc. ISMRM*, pp. 2256, 2005.
[6] Xu et al., submitted to *Proc. ISMRM*, 2007.
[7] Xu et al., submitted to *Proc. ISMRM*, 2007.
[8] Medical VR Studio GmbH, *www.vr-laboratory.com.*
[9] Saekho et al., *MRM*, vol. 55, pp. 719-724, 2006